LETTER • OPEN ACCESS

Long-term carbon dioxide removal potential from the application of wood biochar and basanite rock powder in sandy soil using the LiDELSv2 process-based modeling approach

To cite this article: Mikita Maslouski *et al* 2025 *Environ. Res. Lett.* **20** 124032

View the article online for updates and enhancements.

ENVIRONMENTAL RESEARCH
LETTERS

LETTER

Check for updates

Long-term carbon dioxide removal potential from the application of wood biochar and basanite rock powder in sandy soil using the LiDELSv2 process-based modeling approach

Mikita Maslouski[1,*], Maria Ansari[2], Susanne E Hamburger[3], Johannes Meyer zu Drewer[4,5,6], Nikolas Hagemann[4,6,7], Annette Eschenbach[2], Christian Beer[2], Joscha N Becker[2], Claudia I Kammann[3], Maria-Elena Vorrath[8] and Philipp Porada[1]

1 Institute of Plant Science and Microbiology, University of Hamburg, Hamburg, Germany
2 Department of Earth System Sciences, University of Hamburg, Hamburg, Germany
3 Department of Applied Ecology, Hochschule Geisenheim University, Geisenheim, Germany
4 Ithaka Institute, Goldbach, Germany
5 Institute for Sustainable Energy Systems, Offenburg University of Applied Sciences, Offenburg, Germany
6 Agroscope, Zürich, Switzerland
7 Ithaka Institute, Arbaz, Switzerland
8 Institute for Geology, University of Hamburg, Hamburg, Germany
* Author to whom any correspondence should be addressed.

E-mail: mikita.maslouski@uni-hamburg.de

Abstract

The rise in atmospheric carbon dioxide (CO_2) concentrations requires scalable and effective carbon dioxide removal (CDR) strategies. pyrogenic carbon capture and storage relies on the pyrolysis of biomass and the non-oxidative use of biochar, e.g. in soils. Enhanced rock weathering (ERW) captures CO_2 by forming dissolved bicarbonate. In addition to CDR, both methods may offer soil improvement as a co-benefit. However, their interaction and combined CDR potential remain largely unexplored. Here, we investigate their individual and combined effects on carbon dynamics in a temperate agricultural soil. Using the process-based LiDELSv2 model calibrated against data from the lysimeter experiment, we simulate 1000 year impacts of applying 4.2 wt% wood biochar, 2 wt% basanite rock powder (RP), their co-application, and co-pyrolyzed material (rock-enhanced biochar, RE-biochar) on soil organic carbon (SOC), net primary production (NPP), net CO_2 ecosystem exchange (NEE), and calcium (Ca^{2+}) leaching in a northern German sandy soil. Biochar alone led to the highest increase in SOC and achieved a modeled NEE of $-200\,\mathrm{g\,C\,ha^{-1}\,yr^{-1}}$ per ton of biochar throughout 1000 years, acting as a long-term carbon sink. Co-application and RE-biochar increased SOC too, but to a lesser extent. Rock powder alone reduced SOC by 7%. Although RP enhanced Ca^{2+} leaching, this did not result in net CO_2 removal. Ecosystem respiration and NPP remained stable in the long term. Our results suggest that, when accounting for assumed application rates, biochar is the primary driver of long-term soil-based CDR, while ERW provides only minor co-benefits. This highlights the need to tailor interventions to specific soil and climate conditions.

1. Introduction

Climate change is primarily driven by the increase in atmospheric carbon dioxide (CO_2), resulting largely from anthropogenic activities such as fossil fuel combustion, deforestation, and industrial processes. During the past two centuries, CO_2 emissions have far exceeded the Earth's natural capacity to absorb them, leading to global warming and wide-ranging impacts on biodiversity, human health, food security, and ecological stability (Al-Ghussain 2019, Calvin *et al* 2023, Keerthi 2024).

Although emission reduction is and will remain critical, carbon dioxide removal (CDR) approaches

are increasingly recognized as an essential additive strategy to limit the global rise in temperature (Calvin *et al* 2023, Smith *et al* 2024). These approaches aim to actively remove CO_2 from the atmosphere and securely store it over long timescales (Calvin *et al* 2023, Keerthi 2024).

Within CDR strategies, pyrogenic carbon capture and storage (PyCCS) involves the production of biochar, a stable, carbon rich product derived from biomass non-oxidative pyrolysis, and its application to soils for long-term carbon sequestration. In the soil, biochar might stabilize carbon and prevents rapid decomposition (Schmidt *et al* 2019). Hence, biochar application increases soil organic carbon (SOC) stocks by stabilizing biomass-derived carbon and, potentially, by increasing plant-derived C inputs by stimulating plant growth and yields (Schmidt *et al* 2021). The labile carbon fraction of biochar (3%–30%) is decomposed by soil microorganisms, releasing nutrients that support plant growth when produced from nutrient-rich feedstock (Archontoulis *et al* 2016). Moreover, biochar can improve soil water retention, and overall soil fertility, potentially enhancing CO_2 uptake through increased biomass productivity (Lehmann *et al* 2021, Schmidt *et al* 2021, Acharya *et al* 2024) and it can also reduce agricultural emissions of non-CO_2 greenhouse gases (Lehmann *et al* 2021). First long-term studies in biochar-amended agricultural soils reported an increase in overall SOC stocks (Blanco-Canqui *et al* 2020, Weng *et al* 2022, Guo *et al* 2024). However, findings from Gross *et al* (2024) report no increase in SOC stock.

Enhanced rock weathering (ERW) is another CDR process that accelerates the natural weathering of silicate minerals to capture atmospheric CO_2 and form bicarbonate in the aqueous phase or carbonate minerals in the solid phase, both stable for at least 10 000 years (Hartmann *et al* 2013, Renforth and Henderson 2017). Beyond carbon sequestration, this approach can also improve soil structure, enhance nutrient availability, and contribute to SOC stabilization (Buss *et al* 2022, Dupla *et al* 2024). Like biochar, ERW may support increased CO_2 uptake by vegetation through improved soil fertility and plant growth (Swoboda *et al* 2022, Dupla *et al* 2024).

Although the individual effects of biochar and rock powder (RP) on soil and carbon dynamics are well documented (Hartmann *et al* 2013, Schmidt *et al* 2021), their combined application remains relatively understudied. Biochar may enhance rock weathering by improving soil aeration and stimulating microbial activity, potentially accelerating geochemical reactions (Amann and Hartmann 2019). In contrast, under certain conditions—such as in compacted soils or when biochar with fine particle size is applied at high rates—it can suppress weathering by clogging pore spaces and increasing soil hydrophobicity, thus limiting water–mineral interactions (Obia *et al* 2017,

Vitková *et al* 2024). A nine-week field lysimeter experiment showed that, when co-applied with basanite, biochar was the dominant driver of changes in soil carbon content and microbial activity (Ansari *et al* n.d.). In contrast, Honvault *et al* (2024) suggest that while plant biomass production and nutrient availability were generally additive under co-application, these effects were largely driven by the basalt amendment. In both cases (Honvault *et al* 2024, Ansari *et al* n.d.), the dominant role of either amendment may also be linked to its considerably higher application rate, potentially influencing the relative strength of biochar or RP effects.

Most existing experimental studies have focused on short-term responses of biochar–RP combinations and their potential additive or synergistic CDR effects (Honvault *et al* 2024, Vorrath *et al* 2025, Ansari *et al* n.d., Hamburger *et al* n.d.). However, the stability of these amendments and their interactions must be understood over much longer timescales to reliably assess their net CDR potential. To address this gap, we employed the LiBry-DETECT Layers Scheme version 2 (LiDELSv2) – a process-based model that simulates the effects of biochar and RP on soil properties, both individually and in combination, over centennial to millennial timescales.
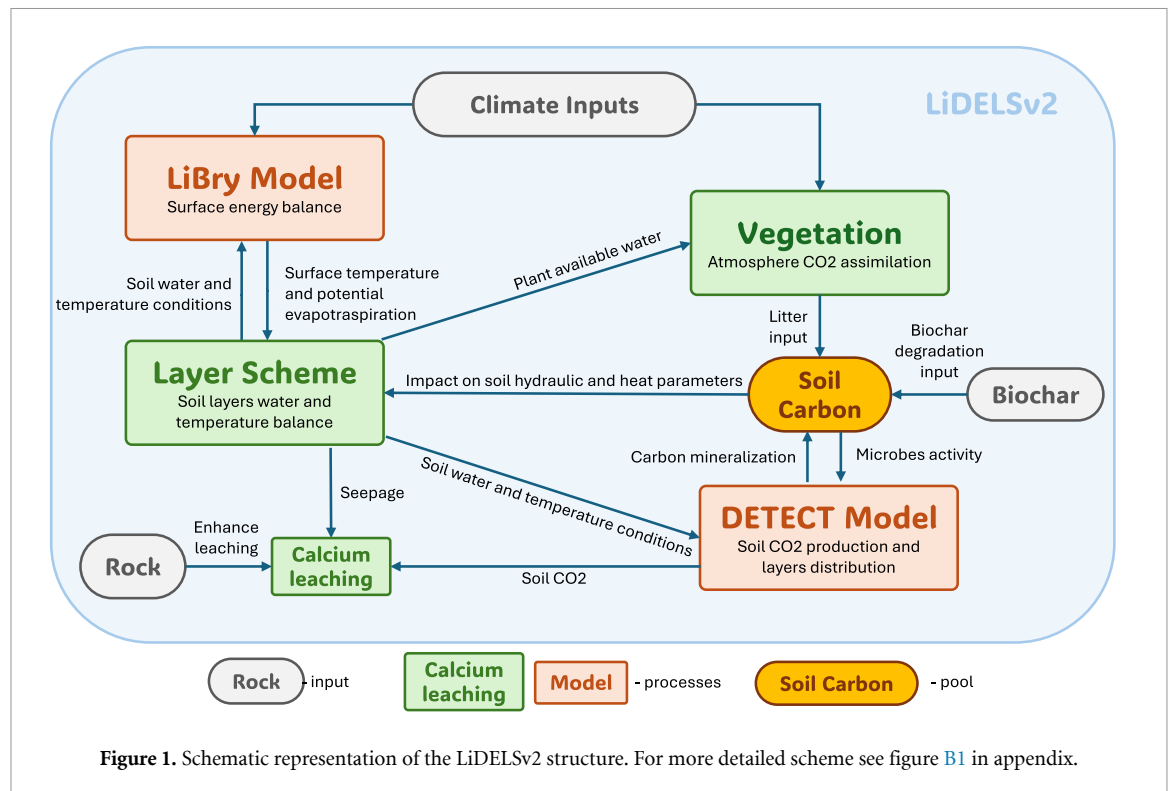
In this study, we used LiDELSv2 to investigate the cumulative carbon removal potential over 1000 years from the sole, co-application and co-pyrolysis of wood-derived biochar and basanite RP in a sandy soil under northern German climatic conditions.

2. Materials and methods

2.1. Geisenheim experiment

The calibration of the LiDELSv2 was based on a lysimeter experiment conducted on the grounds of Hochschule Geisenheim University, Germany (49°59′1″N, 7°57′22″E). The experiment used a sandy agricultural topsoil of northern Germany, sourced from Gräflich Bernstorff'sche Betriebe, Gartow (53°1′10″N, 11°30′01″E), with a texture comprising 93.8% sand and 2.5% silt. The soil was placed in lysimeter pots and amended with different combinations of biochar and/or basanite RP (Ansari *et al* n.d., Hamburger *et al* n.d.). Cabbage turnip (*Brassica oleracea* var. *gongylodes* L.) was cultivated as the test crop (Hamburger *et al* n.d.).

The biochar used in this experiment was produced from wood chips at 650 °C (hereafter referred to as wood biochar (WB)). The basanite RP (commercial name: *Eifelgold*) was sourced from Rheinische Provinzial-Basalt- und Lavawerke, Sinzig, Germany (hereafter referred to as RP. Rock-enhanced biochar (RE-biochar) was produced from a mixture of wood chips and basanite in a weight ratio of 80:20, followed by pelletization and pyrolysis at 650 °C at industrial scale. The resulting RE-biochar consisted

Figure 1. Schematic representation of the LiDELSv2 structure. For more detailed scheme see figure B1 in appendix.

of approximately 68% biochar and 32% basanite by weight. The same ratio (2.1:1) was assumed for the co-application of biochar and basanite. Further details on the (RE-)biochars are provided in Meyer zu Drewer and Hagemann (2025), while the properties of the basanite RP are described in Meyer zu Drewer *et al* (2025).

The soil in the lysimeter pots was mixed with WB at a 4.2% weight-to-weight ratio (wt%), corresponding to an application rate of approximately 120 t ha^{-1}. For the sole RP treatment, the application rate was 2 wt%, equivalent to 57 t ha^{-1}. The RE-biochar treatment was applied at 6.2 wt%, corresponding to 177 t ha^{-1}. In the co-application treatment, the soil was mixed with 4.2 wt% of biochar and 2 wt% of basanite RP (Ansari *et al* n.d., Hamburger *et al* n.d.).

At the end of the experiment, Ansari *et al* (n.d.) measured soil water retention parameters, bulk density (table 1), SOC content, microbial biomass (MB) and Hamburger *et al* (n.d.) measured cumulative crop yield. These measurements were subsequently used for model calibration (see sections A.1–A.3 in appendix).

2.2. LiDELSv2 process-based modeling approach

LiBry-DETECT Layer Scheme version 2 (LiDELSv2, figure 1) is a one-dimensional, process-based ecosystem model that integrates soil–plant–atmosphere interactions under biochar and mineral amendment scenarios (Maslouski *et al* 2025). It is based on two earlier models: LiBry (Porada *et al* 2013), which simulates energy and water fluxes at the

soil-atmosphere interface, and DETECT (Ryan *et al* 2018), which calculates soil CO_2 production and vertical transport. The soil is modeled in discrete layers, allowing for dynamic simulation of heat and water transport, soil carbon dynamics, changing hydraulic conductivity, and thermal capacity due to amendments. Vegetation processes are modeled via light- and CO_2-limited photosynthesis (Farquhar *et al* 1980) and stomatal regulation based on root-zone water availability (Bonan 2019). The model has been previously validated for sandy soils under northern German climatic conditions and accurately reproduces key biogeophysical processes (Maslouski *et al* 2025).

Compared to previous version by Maslouski and Porada (2024), LiDELSv2 now includes several key developments. First, a soil evaporation module based on Bonan (2019) was implemented, allowing for a more realistic representation of soil water fluxes beyond transpiration alone. In the reference scenario, this component accounted for ∼11% of evapotranspiration, consistent with regional observations (Miralles *et al* 2025). Second, a weathering module based on Arens and Kleidon (2008) was added to estimate calcium ion (Ca^{2+}) leaching from silicate minerals. The modeled Ca^{2+} leaching rate was approximately 0.7 g m^{-2} yr^{-1}, which matches empirical estimates for the region (Arens and Kleidon 2011). Finally, a biochar degradation module was incorporated to simulate the gradual breakdown of labile biochar fractions, using decay rates for oak biochar produced at 650 °C from Zimmerman (2010). This module affects soil carbon dynamics,

Table 1. Soil and amendment parameters used as model inputs. Values obtained from the Geisenheim experiment (Ansari *et al* n.d.) are presented as treatment means $\pm$ standard deviation ($n = 0.05$). Different letters within a row indicate statistically significant differences between treatments ($p < 0.05$). Note that Meyer zu Drewer and Hagemann (2025) did not report statistical analyses for the carbon (C) content of the amendments. The persistent aromatic carbon fraction (PAC) was not measured for the (RE-)biochar used in this study and was therefore assumed from the BC_{HyPy} fraction of a comparable material (same rock type and amendment rate, similar feedstock and pyrolysis conditions at pilot scale, Meyer zu Drewer *et al* (2025)). This values is also consistent with recently published PAC dependencies on production conditions by Hagemann *et al* (2025).

Treatment parameter	Control	Rock powder (RP)	Wood biochar (WB)	Co-application RP + WB	Co-pyrolysis (RE-biochar)
Bulk density ($g\,cm^{-3}$)	1.26 ± 0.03^a	1.26 ± 0.04^a	1.14 ± 0.03^b	1.17 ± 0.04^c	1.21 ± 0.03^d
Porosity (—)	0.51 ± 0.01^a	0.52 ± 0.02^a	0.56 ± 0.01^b	0.55 ± 0.02^b	0.53 ± 0.01^c
Saturated conductivity ($cm\,h^{-1}$)	43 ± 4^a	50 ± 18^b	47 ± 4^a	52 ± 7^a	47 ± 4^a
van Genuchten α (cm^{-1})	0.031 ± 0.005^{ab}	0.029 ± 0.001^a	0.029 ± 0.003^a	0.027 ± 0.001^b	0.028 ± 0.002^{ab}
van Genuchten n (—)	4.9 ± 0.6^a	5.3 ± 0.1^a	4.9 ± 0.4^a	5.6 ± 0.6^a	5.3 ± 0.6^a
C content (—)	0.0124	0.0124**	0.494*	0.494*	0.336*
PAC fraction (—)	n.d	n.d	0.908*	0.908*	0.911*

[*] Indicates the content in the amendments. The soil content value accounts to the sum of control soil and the application rate, which is 4.2 wt% for biochar-related treatments.
[**] Indicates the carbon content in the control.

hydrology, thermal properties (Lawrence and Slater 2008), and microbial activity (Liddle *et al* 2020).

2.3. Model setup

For the model simulations, we used the ECMWF ERA5 climate dataset (Hersbach *et al* 2020) for Hamburg in Germany, which provides 40 years of hourly meteorological data starting from 01 January 1979. For spin up period, model was run for 500 years, repeating the ERA5 dataset, in order to achieve stable state. To simulate long-term dynamics, the dataset then was repeated 25 times to construct a continuous 1000 year climate input for all scenarios, which extrapolate the present climate into the future.

The long-term LiDELSv2 simulations were initialized using measured data from the Geisenheim experiment, which contained soil water retention parameters estimated using the LABROS software based on retention curve measurements from soil samples and information about applied amendments (table 1)

The modeled soil column had a depth of 4 m, with uniform soil parameters corresponding to the control treatment (table 1). For the biochar and/or RP treatments, soil parameters were changed in the top two layers, comprising a cumulative depth of 25 cm, based on the values specified in table 1.

Soil carbon, microbes, and root distributions followed the vertical profiles proposed by Ryan *et al* (2018) in DETECT model. The majority of SOC and MB were concentrated within the top 1 m of the soil profile. Initial SOC values for all scenarios were based on measurements from the Geisenheim experiment and amounted to 67 Mg ha^{-1}. Initial MB was estimated using the calibration relationship described in appendix A.2 section and was set to 8 kg ha^{-1}.

For the biochar degradation, its carbon content and the PAC fraction were used (table 1). PAC is defined as the fraction of biochar carbon that remains stable in the soil for over 1000 years (Schmidt *et al* 2024). From a modeling perspective, only the labile fraction of (RE-)biochar—calculated as (1 - PAC) – contributes to degradation. Within this labile part, only the (RE-)biochar's carbon content (table 1) contributes to the SOC pool.

For the calcium leaching module, we applied the sandstone lithology class proposed by Arens (2013) (after Nockolds 1954) for the control treatment. For treatments containing RP, the control lithology was adjusted using a weighted average with the basalt lithology class from Arens (2013).

To approximate the effects of lower, more agronomically realistic biochar application rates, we scaled the amendment-induced changes in soil parameters (table 1) linearly relative to the control. Specifically, the difference between the control and a given treatment was reduced in proportion to the assumed application rate. For example, the porosity in the WB treatment ($\rho = 0.56$) differs from the control ($\rho = 0.51$) by 0.05 at the applied rate of 4.2 wt%. At half this rate, the adjustment was reduced to 0.025, yielding a porosity of 0.535, while at one-quarter of the rate it was 0.0125, resulting in 0.5225. The same procedure was applied to saturated conductivity, bulk density, and the van Genuchten parameters.

3. Results

3.1. Effects on SOC pool

For the control treatment, LiDELSv2 applies a steady-state approach, where SOC remains nearly constant throughout the simulation (table 2). For treatments containing biochar, we distinguish between total SOC (SOC_{total}), representing the sum of SOC and biochar, and non-biochar SOC (SOC_{nonBC}), which excludes both the PAC fraction and the labile portion of biochar that has not yet decomposed (turned into SOC_{nonBC}) at a given point in time. Only SOC_{nonBC} (denoted as $c_{o,soil}$ in figure B1 in the appendix) affects the dynamic processes in the model, including soil heat fluxes, water balance, and microbial activity.

The highest cumulative increase in SOC_{nonBC} of approximately 52% compared to the control was observed for the sole application of WB (figure 2) in 1000 years. When normalized by application rate, this corresponds to an increase in SOC_{nonBC} by ~ 308 kg C ha^{-1} yr^{-1} per ton of applied biochar. This was followed by the WB+RP and RE-biochar treatments, which resulted in SOC_{nonBC} increases of 17% and 10%, respectively. These changes were most pronounced during the first 500 years of the simulation, with the accumulation rate gradually declining thereafter. In contrast, the sole application of RP led to a consistent reduction in SOC_{nonBC}, reaching a decrease of 7% over the 1000 year period.

Sole WB application and its co-application with RP resulted in the largest increases in SOC_{total} of approximately 154% and 121% above control levels after 500 years, respectively (figure 3). The RE-biochar treatment, characterized by a lower carbon content, produced a more moderate increase of 81% after 500 years. For the control and RP-only treatments, SOC_{total} corresponds directly to SOC_{nonBC}, due to the absence of biochar.

3.2. Effects on CO$_2$ fluxes

As mentioned earlier, SOC in LiDELSv2 remains nearly constant, reflecting a long-term balance between CO$_2$ assimilation and ecosystem respiration (R_{eco}) in the control treatment. Since LiDELSv2 does not account for changes in nutrient dynamics, modeled CO$_2$ fluxes may vary as a result of changes in soil temperature and hydrology, which in turn affect microbial and plant activity.

The most notable change in net primary production (NPP) occurred during the early years following biochar application (figure 4). Over time, changes in SOC and soil properties had only minor impacts on vegetation productivity (table 3), and NPP remained relatively stable across all treatments. Biochar sole treatment showed a modest 1% increase in NPP, while RP-alone decreased NPP by 0.4%. Co-application and co-pyrolysis treatments showed negligible changes ($\pm 0.1\%$) relative to the control.

Model results did not show significant changes in R_{eco} (table 4). Biochar-related treatments initially decreased CO$_2$ release, with the largest reduction observed in the WB-only scenario—a 1.3% decrease during the first 50 years compared to control. However, this effect diminished over time, resulting in up to 0.3% over 1000 years (figure 5). The RP-only treatment showed a 0.1% increase in CO$_2$ respiration in the first 50 years, followed by a 0.2% decrease compared to control over the next 500 years.

To estimate the net CO$_2$ balance of the modeled ecosystem with and without amendments, we calculated the net ecosystem exchange (NEE) as the difference between R_{eco} and gross primary production (table 5). In the first 300–400 years, all biochar-related treatments reduced NEE relative to the control (figure 6). However, over longer timescales, NEE in both the co-application and co-pyrolysis scenarios became indistinguishable from the control, making their long-term impact comparable to the baseline.

In contrast, the WB-only treatment consistently maintained lower NEE values than the control, resulting in a net CO$_2$ removal of approximately 24 kg C ha^{-1} yr^{-1} over the 1000 year period. When normalized by application rate, this corresponds to ~ 200 g C ha^{-1} yr^{-1} per ton of applied biochar. The RP-only treatment resulted in higher NEE values, primarily due to reduced carbon assimilation caused by lower soil moisture. These results suggest that, under the modeled conditions, RP does not meaningfully contribute to long-term reductions in CO$_2$ emissions.

3.3. Effects on calcium leaching

In our weathering model, Ca^{2+} as the dominant cation released during the dissolution of basanite was assumed to be mobilized into soil groundwater and exported via drainage, representing a potential long-term CDR pathway. While the model focused on Ca^{2+}, other cations such as Mg^{2+}, K$^+$, and Na$^+$ may also participate in weathering reactions and enhance CO$_2$ removal, although they were not explicitly modeled.

Calcium leaching increased in all RP-containing treatments, indicating enhanced weathering activity (table 6). The strongest response (figure 7) was seen in the RP-only treatment, with a 21% increase in Ca^{2+} release in the short-term that gradually declined over time to 19%. Assuming the formation of 2 moles of HCO$_3^-$ per mole of Ca^{2+} leached, the additional CDR potential from leaching may reach up to ~ 3 g CO$_2$ ha^{-1} yr^{-1}, representing a theoretical upper bound.. Co-application and co-pyrolysis scenarios showed similar but slightly weaker effects ($\sim 14\%$ short-term, declining to $\sim 8\%$ in the long term). In contrast, WB-only treatment led to a reduction in Ca^{2+} leaching—up to 26% at 1000 years—mainly due to reduced soil water movement, which is a key driver of calcium leaching in the LiDELSv2.

Table 2. Mean non-biochar (nonBC) and total soil organic carbon in kg C m^{-2} for each treatment, averaged over specific time intervals and expressed relative to the control soil column. Values represent treatment means $\pm$ standard deviation. All treatments within a column differ significantly from one another ($p < 0.05$).

Timeframe	0–50 yrs		51–100 yrs		101–500 yrs		501–1000 yrs	
Treatment	nonBC	total	nonBC	total	nonBC	total	nonBC	total
Control	6.9 ± 0.2		6.7 ± 0.2		6.2 ± 0.2		7.1 ± 0.6	
Rock powder (RP)	6.8 ± 0.2		6.5 ± 0.2		5.8 ± 0.3		6.6 ± 0.6	
vs control (%)	−1		−3		−6		−7	
Wood biochar (WB)	7.7 ± 0.3	14.3 ± 0.3	8.5 ± 0.2	15.0 ± 0.2	9.4 ± 0.3	15.6 ± 0.3	10.8 ± 0.7	17.0 ± 0.7
vs control (%)	+13	+109	+27	+123	+52	+154	+52	+138
Co-application (RP + WB)	7.3 ± 0.2	13.9 ± 0.2	7.5 ± 0.1	14.0 ± 0.2	7.3 ± 0.2	13.6 ± 0.2	8.3 ± 0.6	14.5 ± 0.7
vs control (%)	+7	+103	+12	+108	+19	+121	+17	+104
Co-pyrolysis (RE-biochar)	7.1 ± 0.2	11.6 ± 0.2	7.2 ± 0.1	11.6 ± 0.2	6.9 ± 0.2	11.1 ± 0.3	7.8 ± 0.6	12.1 ± 0.6
vs control (%)	+4	+69	+7	+73	+11	+81	+10	+70
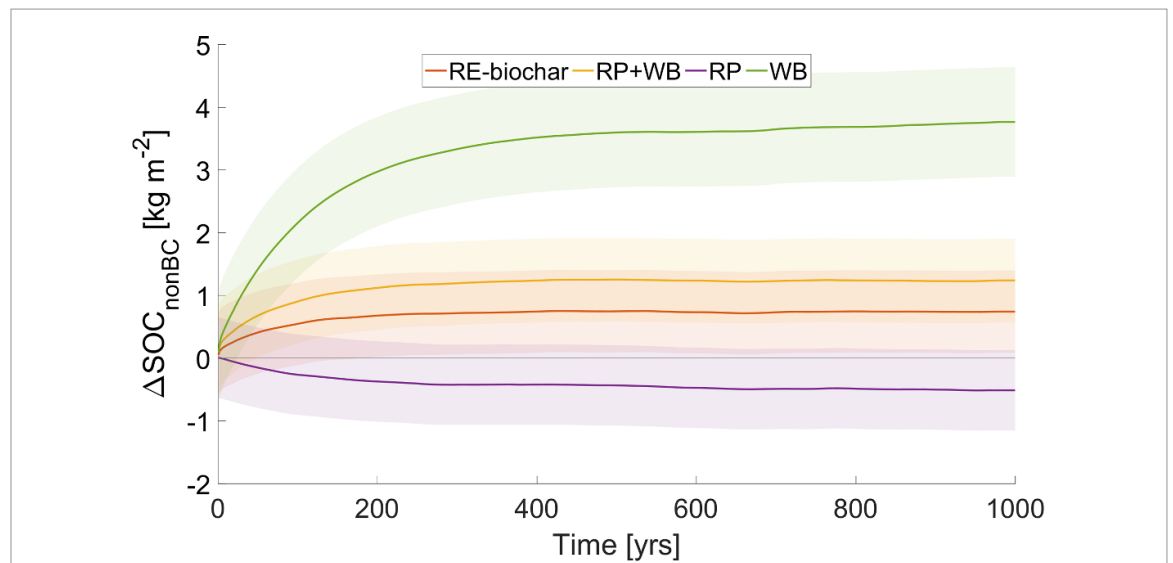
Figure 2. Change in mean non-biochar soil organic carbon relative to the modeled control treatment (ΔSOC_{nonBC}) for wood biochar (WB), rock powder (RP), their co-application (RP+WB), and co-pyrolysis (RE-biochar). Solid lines represent smoothed trends, while shaded areas represent the standard deviation caused by natural ecosystem variability.

Figure 3. Smoothed mean trends of total soil organic carbon relative to the modeled control treatment (ΔSOC_{total}, solid lines) for wood biochar (WB), co-application with rock powder (RP+WB), and their co-pyrolysis (RE-biochar). Shaded areas represent the standard deviation caused by natural ecosystem variability. Dashed colored lines indicate the modeled contribution of biochar to SOC_{total}, while the dashed gray lines show the initial biochar carbon input at the time of application.

Figure 4. Change in mean net primary production over time compared to the modeled control soil column (Δ NPP) for wood biochar (WB), rock powder (RP), their co-application (RP+WB), and co-pyrolysis (RE-biochar). Solid lines represent smoothed trends, while shaded areas represent the standard deviation caused by natural ecosystem variability.

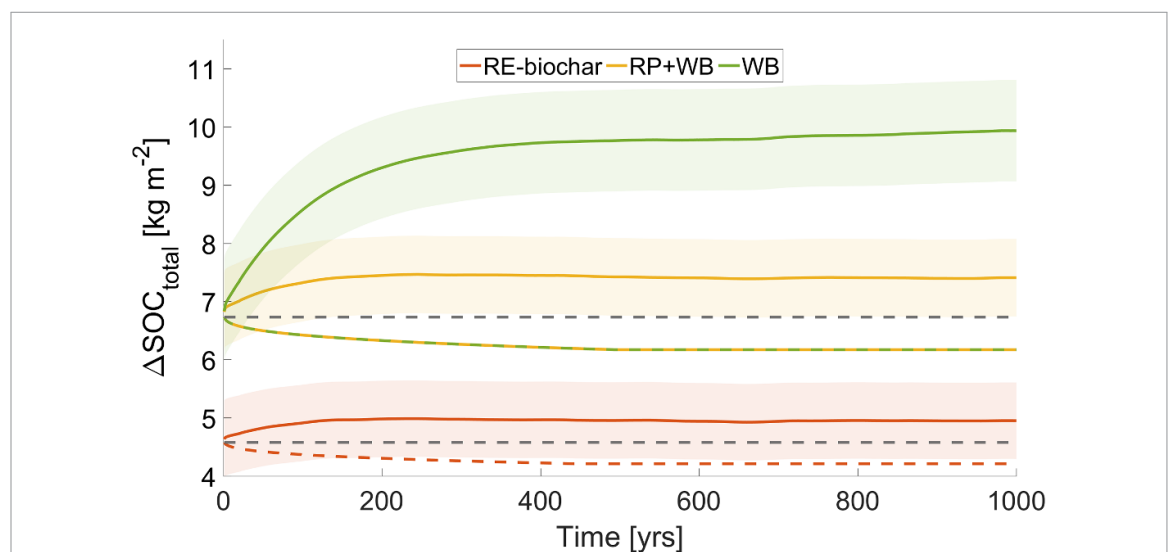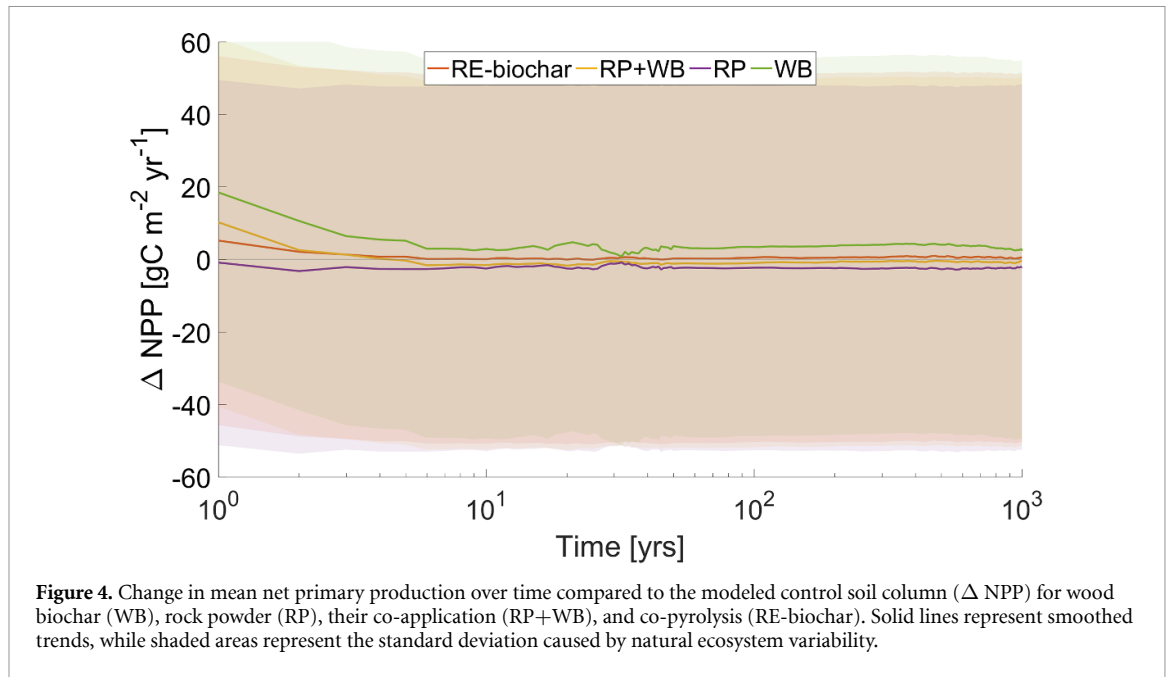**Table 3.** Mean net primary production (NPP) for each treatment, averaged over specific time intervals, and expressed compared to the control soil column. Values represent treatment means $\pm$ standard deviation. All treatments within a column do not differ significantly from one another ($p > 0.05$).

NPP ($g\,C\,m^{-2}\,yr^{-1}$) treatment	0–50 yrs	51–100 yrs	101–500 yrs	501–1000 yrs
Control	577 ± 49	574 ± 49	572 ± 50	585 ± 51
Rock powder (RP) vs control (%)	575 ± 48 −0.3	571 ± 48 −0.4	570 ± 49 −0.4	583 ± 50 −0.4
Wood biochar (WB) vs control (%)	583 ± 55 +1.0	577 ± 50 +0.6	576 ± 52 +0.7	589 ± 54 +0.6
Co-application RP + WB vs control (%)	578 ± 52 +0.2	573 ± 48 −0.2	572 ± 50 −0.1	585 ± 52 −0.1
Co-pyrolysis (RE-biochar) vs control (%)	578 ± 50 +0.2	574 ± 49 +0.1	573 ± 50 +0.1	586 ± 51 +0.1

Table 4. Mean ecosystem respiration (R_{eco}) for each treatment, averaged over specific time intervals, and expressed compared to the control soil column. Values represent treatment means $\pm$ standard deviation. All treatments within a column do not differ significantly from one another ($p > 0.05$).

| R_{eco} ($g\,C\,m^{-2}\,yr^{-1}$) Treatment	0–50 yrs	51–100 yrs	101–500 yrs	501–1000 yrs
Control	1190 ± 76	1201 ± 71	1200 ± 72	1210 ± 72
Rock powder (RP) vs control (%)	1192 ± 76 +0.1	1201 ± 71 0.0	1198 ± 72 −0.2	1208 ± 72 −0.2
Wood biochar (WB) vs control (%)	1174 ± 75 −1.3	1191 ± 71 −0.8	1201 ± 72 +0.1	1213 ± 72 +0.3
Co-application RP + WB vs control (%)	1184 ± 76 −0.5	1197 ± 71 −0.3	1199 ± 72 −0.1	1210 ± 72 −0.1
Co-pyrolysis (RE-biochar) vs control (%)	1187 ± 76 −0.2	1200 ± 71 −0.1	1200 ± 72 0.0	1211 ± 72 0.0
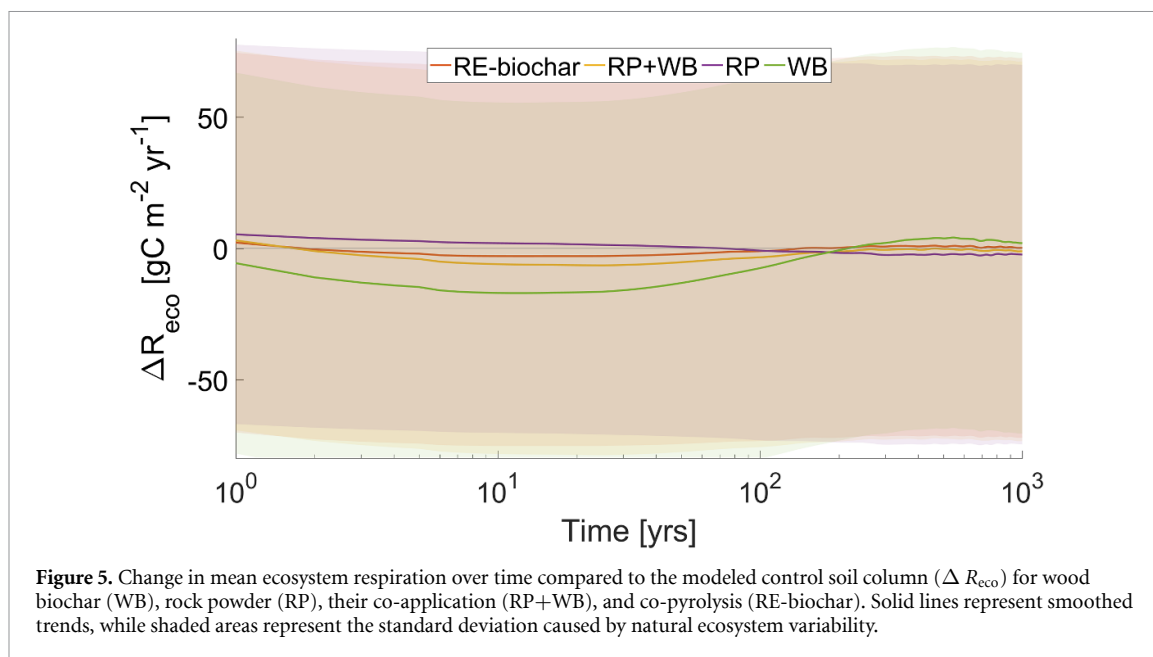
Figure 5. Change in mean ecosystem respiration over time compared to the modeled control soil column (ΔR_{eco}) for wood biochar (WB), rock powder (RP), their co-application (RP+WB), and co-pyrolysis (RE-biochar). Solid lines represent smoothed trends, while shaded areas represent the standard deviation caused by natural ecosystem variability.

Table 5. Mean net ecosystem exchange (NEE) for each treatment, averaged over specific time intervals, and expressed compared to the control soil column. Values represent treatment means $\pm$ standard deviation. All treatments within a column do not differ significantly from one another ($p > 0.05$).

NEE ($g\,C\,m^{-2}\,yr^{-1}$) Treatment	0–50 yrs	51–100 yrs	101–500 yrs	501–1000 yrs	1000 yrs mean
Control	-6 ± 73	3 ± 71	1 ± 71	-2 ± 72	-1 ± 71
Rock powder (RP)	-3 ± 72	5 ± 70	2 ± 70	-2 ± 71	0 ± 70
vs control	$+3$	$+2$	$+1$	0	$+1 \pm 70$
Wood biochar (WB)	-28 ± 79	11 ± 71	-1 ± 73	-3 ± 75	-3 ± 74
vs control	-22	-14	-2	-1	-2 ± 74
Co-application RP + WB	-13 ± 76	0 ± 70	1 ± 71	-2 ± 72	-1 ± 71
vs control	-7	-3	0	0	0 ± 71
Co-pyrolysis (RE-biochar)	-10 ± 74	1 ± 71	1 ± 71	-2 ± 72	0 ± 71
vs control	-4	-2	0	0	0 ± 71

3.4. Sensitivity to biochar application rates

Under the assumed conditions, all biochar-amended treatments exhibited an approximately linear dependence of SOC change on application rate after 100 years (figure 8), with a slight quadratic tendency. For NEE (figure 9), a quadratic response was observed only for the co-application treatment, whereas the WB and RE-biochar treatments showed only small deviations from linearity.

4. Discussion

4.1. Model validity and relevance of application rates

The control scenario assumes a steady-state system with minimal change in SOC over the 1000 year simulation period. The initial SOC stock was set to $67\,t\,ha^{-1}$ based on measurements from the Geisenheim experiment and reached a mean of $71 \pm 6\,t\,ha^{-1}$ during the final 500 years. This value is slightly lower than the mean SOC reported for German mineral soils, which typically ranges from 90 to $100\,t\,ha^{-1}$ (Poeplau *et al* 2020).

Simulated values for NPP in the control scenario averaged 572–$585\,g\,C\,m^{-2}\,yr^{-1}$, aligning well with reported ranges of 590–$680\,g\,C\,m^{-2}\,yr^{-1}$ for temperate croplands under comparable climatic conditions (Ma 2020). The control treatment was constrained to be approximately NEE-neutral ($-1\,g\,C\,m^{-2}\,yr^{-1}$) in order to maintain a steady state, where ecosystem respiration balances gross primary production in long-term. In real-world systems, however, European croplands tend to exhibit slightly positive NEE values (approximately $+17\,g\,C\,m^{-2}\,yr^{-1}$), indicating a gradual loss of SOC over time (Ciais *et al* 2010).

Taken together, the consistency between modeled, observed, and literature-based values for SOC, NPP, and NEE supports the plausibility of the control simulation and strengthens confidence in the model's capacity to simulate treatment effects.
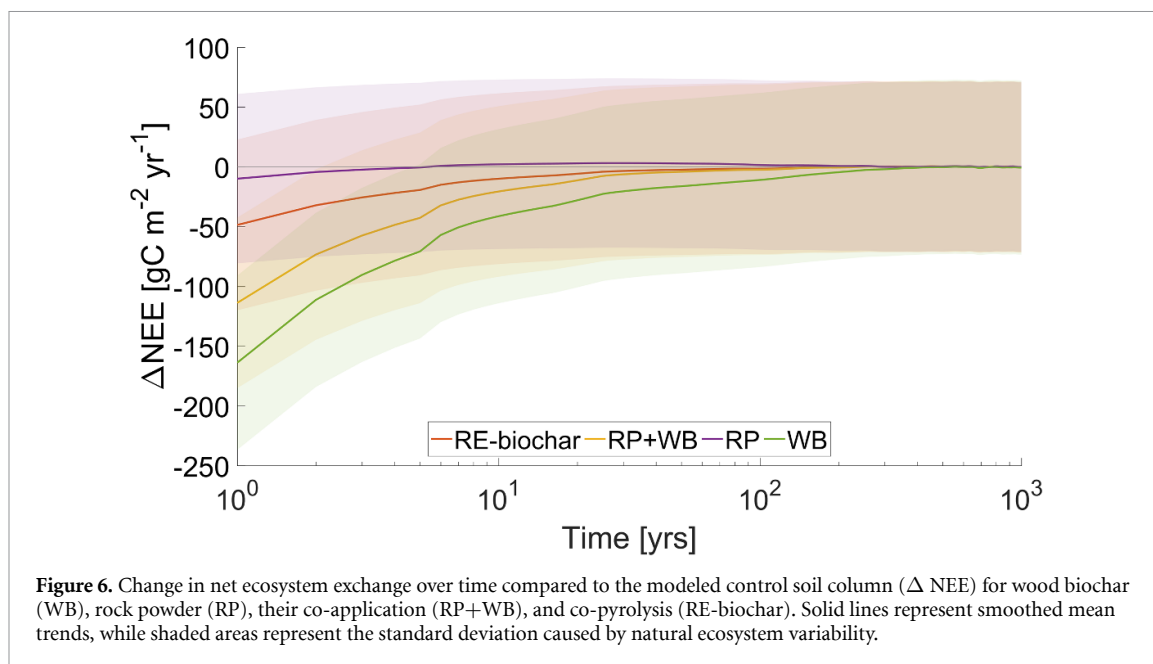
Figure 6. Change in net ecosystem exchange over time compared to the modeled control soil column (Δ NEE) for wood biochar (WB), rock powder (RP), their co-application (RP+WB), and co-pyrolysis (RE-biochar). Solid lines represent smoothed mean trends, while shaded areas represent the standard deviation caused by natural ecosystem variability.

Table 6. Mean calcium ions leaching (Ca^{2+}) for each treatment, averaged over specific time intervals, and expressed compared to the control soil column. Values represent treatment means $\pm$ standard deviation. Different letters within the same column indicate statistically significant differences between treatments ($p < 0.05$).
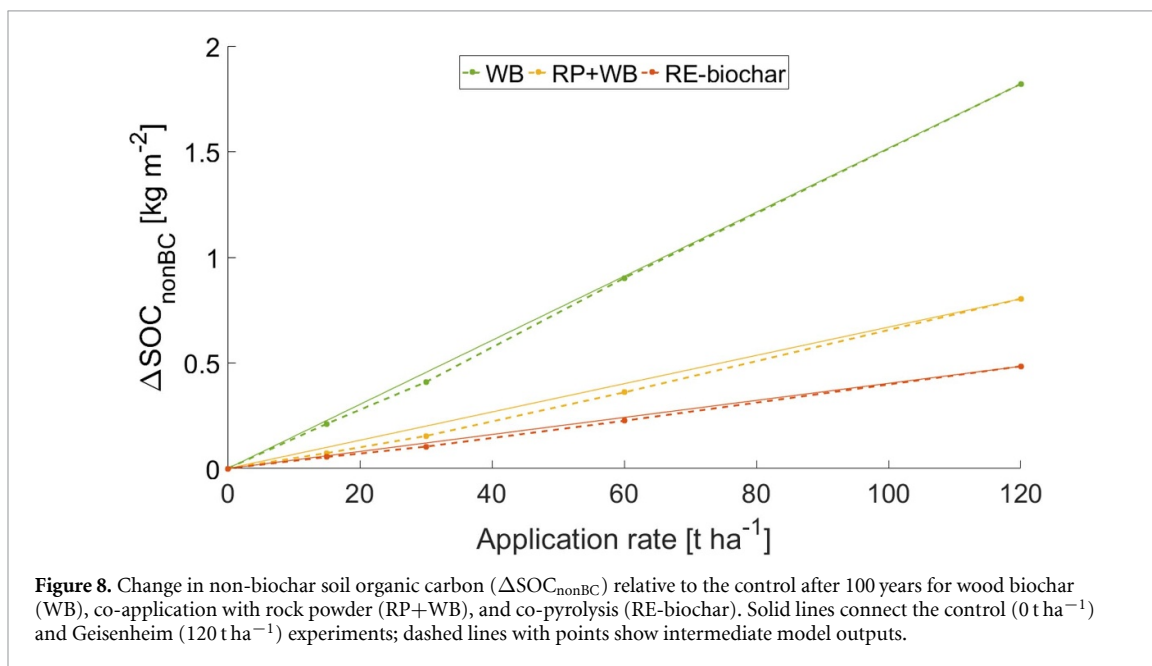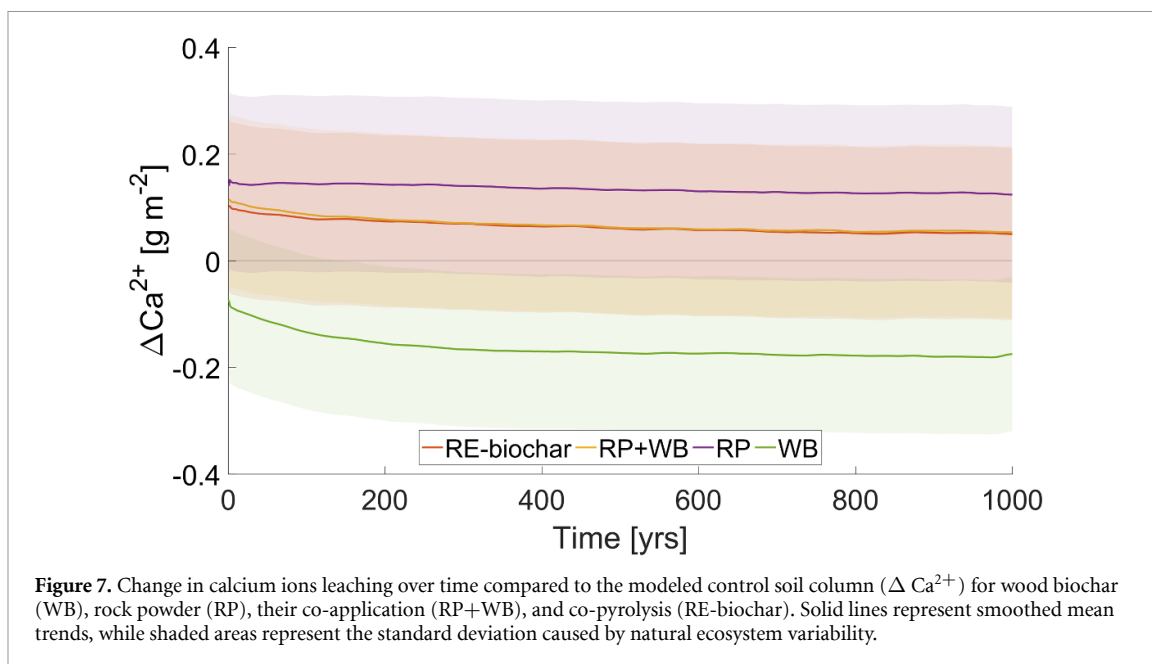
Ca^{2+} ($g\,m^{-2}\,yr^{-1}$) Treatment	0–50 yrs	51–100 yrs	101–500 yrs	501–1000 yrs
Control	0.69 ± 0.14^a	0.68 ± 0.15^a	0.70 ± 0.15^a	0.67 ± 0.15^a
Rock powder (RP) vs control (%)	0.83 ± 0.17^b +21	0.83 ± 0.18^b +21	0.84 ± 0.18^b +20	0.80 ± 0.18^b +19
Wood biochar (WB) vs control (%)	0.59 ± 0.13^c −15	0.56 ± 0.14^c −18	0.5 ± 0.13^c −23	0.50 ± 0.13^c −26
Co-application RP + WB vs control (%)	0.79 ± 0.16^b +15	0.78 ± 0.17^b +13	0.78 ± 0.17^d +10	0.73 ± 0.17^d +8
Co-pyrolysis (RE-biochar) vs control (%)	0.77 ± 0.16^b +13	0.76 ± 0.17^b +12	0.77 ± 0.17^d +10	0.73 ± 0.17^d +8

While the modeled biochar and RP application rates in this study were selected to match those used in the Geisenheim experiment, their real-world applicability should be carefully contextualized. The applied rate of 56 t ha^{-1} for RP lies at the upper end of what is considered agronomically feasible (Dietzen *et al* 2018, Beerling *et al* 2020). In contrast, the modeled biochar application rate of 121 t ha^{-1} is well above typical field applications, which generally fall in the range of 10–30 t ha^{-1} (Bekchanova *et al* 2024), which in practice rather will be the result of repeated application of biochar-treated manure or biochar-based fertilizers (Grafmüller *et al* 2024). High biochar application rates can lead to the accumulation of potentially toxic trace elements originating from both biochar and RP and may pose risks when applied to soils (Dupla *et al* 2023, Kujawska 2023). In the RE-biochars comparable to those used in this study, most trace element concentrations (e.g. Zn, Cu) were within EU fertilizer safety standards, although some elements such as Ni approached threshold values (Meyer zu Drewer *et al* 2025). In addition, high application rates may induce hydrophobic soil behavior, potentially reducing surface water infiltration (Vitková *et al* 2024).

These considerations underscore the mechanistic nature of our study: the selected application rates are not intended as direct field recommendations but rather to illustrate long-term system behavior and treatment interactions. While relative changes compared to the control treatment provide meaningful insight, we also present maximum CDR effects normalized to per-ton application rates of biochar, to improve comparability and guide future implementation strategies.

Within this framework, our assumption of linear scaling in soil parameters with decreasing biochar application rates produced nearly linear long-term responses of SOC and NEE across all treatments.

Figure 7. Change in calcium ions leaching over time compared to the modeled control soil column ($\Delta\,Ca^{2+}$) for wood biochar (WB), rock powder (RP), their co-application (RP+WB), and co-pyrolysis (RE-biochar). Solid lines represent smoothed mean trends, while shaded areas represent the standard deviation caused by natural ecosystem variability.

Figure 8. Change in non-biochar soil organic carbon (ΔSOC_{nonBC}) relative to the control after 100 years for wood biochar (WB), co-application with rock powder (RP+WB), and co-pyrolysis (RE-biochar). Solid lines connect the control ($0\,t\,ha^{-1}$) and Geisenheim ($120\,t\,ha^{-1}$) experiments; dashed lines with points show intermediate model outputs.
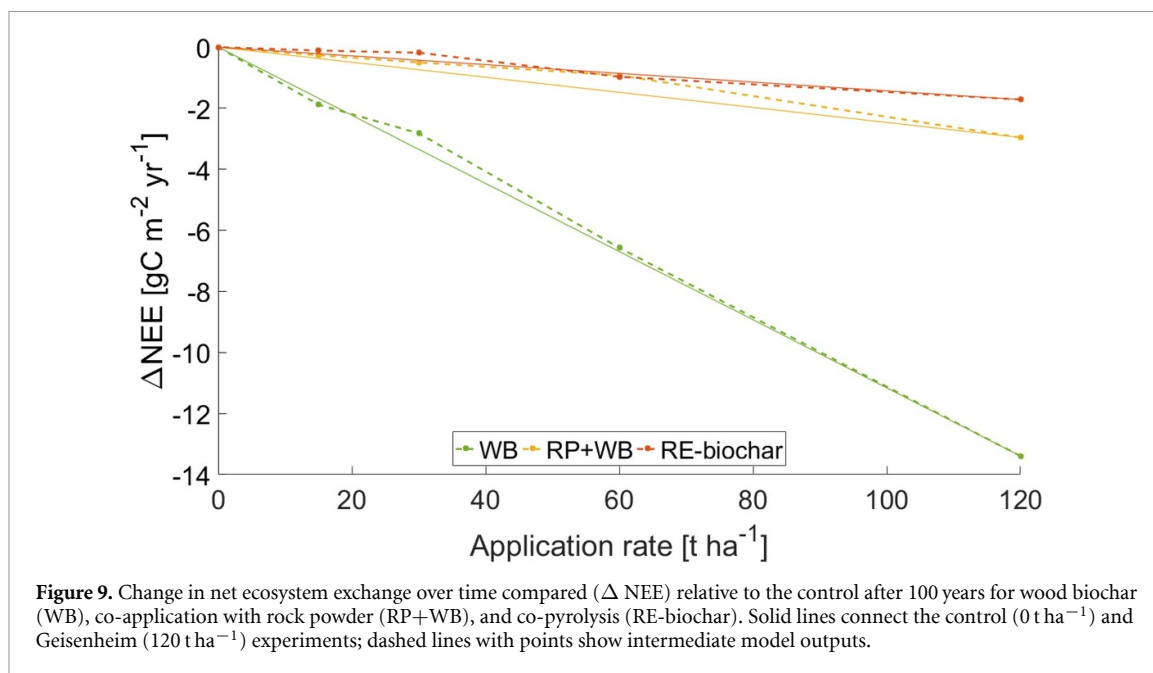
This outcome reflects the simplified parameterization procedure, rather than a mechanistic representation of biochar-soil interactions. In practice, experimental evidence suggests that biochar effects on soil properties and ecosystem fluxes are often nonlinear. Several meta-analyses report near-linear responses of bulk density and porosity to application rate (Blanco-Canqui 2017, Jiang *et al* 2025), but mixed or site-specific effects on saturated conductivity. Blanco-Canqui (2017) further noted that small application rates ($<10\,t\,ha^{-1}$) may produce no measurable change, while high rates ($>2\,wt\%$) do not further reduce soil bulk density. Similarly, Altdorff *et al* (2019) found nonlinear responses of van Genuchten parameters and saturated conductivity across different application levels or repeated application.

Thus, while our model-based results help contextualize potential outcomes at agronomically relevant rates, they should be interpreted as first-order approximations that do not capture the full range of nonlinear feedbacks reported in experimental studies.

4.2. Comparison of (RE-)biochar and RP (co)application

All biochar treatments contributed to increases in modeled SOC_{nonBC} through inputs from labile biochar degradation and from litter derived from increased plant carbon assimilation. It should be noted that the SOC_{nonBC} pool in the model does not retain information about the origin of carbon inputs; whether derived from biochar or litter, all inputs

Figure 9. Change in net ecosystem exchange over time compared (Δ NEE) relative to the control after 100 years for wood biochar (WB), co-application with rock powder (RP+WB), and co-pyrolysis (RE-biochar). Solid lines connect the control (0 t ha^{-1}) and Geisenheim (120 t ha^{-1}) experiments; dashed lines with points show intermediate model outputs.

contribute equally. Subsequent microbial decomposition of SOC_{nonBC} produces CO_2 without distinction of carbon origin. This represents a simplification compared to empirical observations, where biochar degradation may follow distinct oxidation pathways (Zimmerman 2010).

We observed an initial reduction in SOC_{nonBC} losses via soil respiration, until soil carbon stocks grew large enough that R_{eco} increased due to the expanded carbon reservoir (figure 5). In the WB sole scenario, SOC_{nonBC} increased by an average of 13% over the first 50 years and by 52% after 1000 years, relative to the control (table 2).

Most empirical studies cover shorter timescales (typically up to 10 years), a meta-analysis by Gross *et al* (2021) reported a comparable trend, with average SOC increases of 1.3 g C m^{-2}, with higher values observed for longer durations and higher application rates. The slightly lower SOC_{nonBC} and higher SOC_{total} gains in our simulation may reflect the conservative degradation assumptions embedded in the LiDELS model, as well as the properties of high-temperature biochar, which typically contains a smaller labile fraction than low-temperature variants (Tomczyk *et al* 2020).

In contrast, RP application did not directly increase SOC, as it does not introduce carbon into the system. Under field conditions, RP can indirectly enhance SOC by increasing soil pH and nutrient availability, thereby promoting plant growth and litter inputs (Swoboda *et al* 2022, Vienne *et al* 2022). However, these mechanisms are not represented in our model. Instead, the RP treatment was defined by higher saturated hydraulic conductivity and a van Genuchten n parameter, along with a lower van Genuchten α compared to the control (table 1). These properties made the soil slightly more conductive to

water flow, reducing water retention in the root zone. As a result, plant-available water decreased, leading to reduced carbon assimilation and ultimately a 7% decline in SOC over the 1000 year simulation period.

The co-application of WB and RP, as well as the use of RE-biochar, resulted in intermediate outcomes. Both treatments led to increases in SOC relative to the control, but their performance was significantly lower than that of WB alone, despite identical biochar application rates. Even when combining the individual effects of WB and RP, the resulting SOC increase remained higher than that of the WB+RP and RE-biochar treatments. This divergence widened over time, suggesting that co-application or co-pyrolysis may dilute the long-term carbon sequestration benefits of biochar.

Due to the addition of the PAC fraction, SOC_{total} increased substantially under all biochar-related treatments. The high-temperature biochar used in our simulations contained over 90% PAC, resulting in nearly a 100% additional increase in SOC_{total} compared to SOC_{nonBC} for WB and WB+RP treatments, and approximately 60% for RE-biochar. These substantial SOC_{total} gains are expected to remain stable in soil for over a thousand years (Howell *et al* 2022). For low-temperature biochar, a lower fraction of PAC is expected (Hagemann *et al* 2025), resulting in higher proportions of labile carbon that are more rapidly degraded. This would likely lead to greater short-term increases in SOC_{nonBC}, but a reduced potential for long-term carbon storage compared to the high-temperature biochar considered here (Wang *et al* 2016).

All biochar treatments contributed to an increase in NPP, primarily during the first 10 years, driven by improved soil water availability. Over time, as vegetation adapted to the new conditions—represented

in the model by changes in mean annual soil water content—NPP stabilized. Subsequently, the expanded soil carbon reservoir led to an increase in R_{eco}. For WB+RP and RE-biochar, NEE became slightly positive after 300–400 years, offsetting their initial climate benefits over the 1000 year simulation. In contrast, the WB-only treatment consistently maintained lower NEE values than the control, making it the only treatment with a net negative NEE under the modeled conditions.

Our results show that calcium leaching alone does not fully offset the positive NEE observed in the RP-only treatment. However, it provides a modest additional carbon removal effect when RP is co-applied with WB or incorporated into RE-biochar. Findings from Vorrath *et al* (2025), who studied the same basanite rock, suggest that significant contributions to CDR can also arise from other ions present in basanite. These additional weathering reactions may bring the NEE of RP-based treatments closer to that of the control.

Overall, our modeling results align with experimental findings (Vorrath *et al* 2025, Ansari *et al* n.d., Hamburger *et al* n.d.), showing that WB-based scenarios offer the highest CDR potential. Solo biochar application emerges as the primary driver, while weathering-related processes play a secondary, supportive role—mainly through their influence on soil physical and hydrological properties. Vorrath *et al* (2025) also reported that biochar may have up to eight times higher CDR potential than RP. When accounting for applied application rates, this impact could be up to 16 times higher. This disproportion may help explain why our modeling study shows a clear dominance of biochar in terms of long-term carbon sequestration.

4.3. Model limitations

While LiDELSv2 provides a robust and flexible framework for simulating long-term soil carbon dynamics under amendments such as RP and biochar, important mechanistic limitations remain that should be acknowledged and addressed in future model developments.

The model does not represent key processes associated with biochar surface chemistry, such as cation exchange capacity, sorption of organic and inorganic species, or reduction–oxidation reactions. These mechanisms can strongly influence nutrient availability, soil fertility, kinetics of mineral weathering, microbial activity, and influence SOC formation (Joseph *et al* 2021, Lee *et al* 2021, Antonangelo *et al* 2024). Moreover, LiDELSv2 simplifies the weathering module by considering only Ca^{2+} release from basanite, thereby neglecting contributions from other base cations (e.g. Mg^{2+}, K^+, Na^+) and omitting potential interactions between biochar and RP that are mediated by aqueous-phase geochemistry and

reactive transport. As a result, the model likely underestimates or misrepresents the synergistic or antagonistic effects of combined amendments, and our estimates of RP's CDR potential should not be interpreted as a full evaluation of geochemical pathways.

The current version of LiDELSv2 does not simulate nutrient dynamics. In real-world ecosystems, increased nutrient availability can stimulate plant growth and carbon assimilation, potentially enhancing NPP and SOC formation (Li *et al* 2021). As a result, our simulations likely provide a conservative estimate of the CDR potential of the tested amendments, as they focus solely on hydrological and structural soil properties.

Moreover, LiDELSv2 does not account for non-CO_2 greenhouse gas emissions that may be associated with biochar or basalt applications (Joseph *et al* 2021, Chiaravalloti *et al* 2023). These emissions could either offset or enhance the net climate benefit, depending on site-specific conditions and amendment characteristics.

The impact of PAC in the model is represented solely through static soil input parameters. These are assumed to remain unaffected by changes in soil properties, microbial interactions, or long-term weathering processes. In reality, PAC degrades very slowly over centuries, primarily through the gradual breakdown of aromatic structures. This process can alter soil structure and influence modeled soil parameters over time (Mia *et al* 2017), which is not captured in the LiDELSv2.

Finally, the current model run does not include seasonal harvesting, which would in reality increase NEE and reduce SOC stocks over time (Ciais *et al* 2010). Other agricultural practices, such as irrigation, tillage, and fertilization, also influence soil carbon dynamics by altering decomposition rates, microbial activity, and plant productivity (Han *et al* 2024), but are also not represented in the current simulations.

Taken together, these limitations mean that the model results should be interpreted as idealized scenarios that isolate the effects of soil physical and hydrological changes. The exclusion of nutrient cycling, reactive transport, electrochemical processes, management practices, and non-CO_2 emissions implies that the modeled CDR potentials may underestimate or misrepresent real-world outcomes, depending on site conditions. Therefore, while the model provides valuable insights into long-term trends and relative treatment performance, the absolute values of SOC and NEE should be viewed with caution and complemented by empirical data and more comprehensive models in future work.

5. Conclusions

Our long-term simulations using the LiDELSv2 process-based model demonstrate that the

application of biochar to temperate sandy agricultural soil offers the highest potential for CDR and carbon sequestration. Biochar led to persistent increases in both total and non-biochar SOC over a 1000 year period. While co-application with RP and co-pyrolysis also improved SOC stocks, their effectiveness was lower than biochar alone, suggesting that combining biochar with RP may reduce its long-term CDR performance. Rock powder application alone had no positive effect on SOC or NEE, and its CDR potential via enhanced Ca^{2+} leaching was minimal. Across all treatments, modeled impacts on NPP and R_{eco} were small compare to natural ecosystem variation, underscoring that long-term soil-based CDR is primarily driven by the stability of biochar carbon.

The dominant role of biochar can be explained by its $\sim$16 higher CDR potential per unit area compared to RP, based on the application rates used. In the modeled idealized scenario, we refer only to changes in specific soil physical and hydrological properties, and do not simulate nutrient dynamics or non-CO_2 GHG emissions. As such, it likely underestimates the full CDR potential of nutrient-rich amendments. Future modeling efforts should incorporate nutrient cycling, land management practices, and empirical data to refine projections and better guide effective soil-based CDR strategies.

Data availability statement

The data that support the findings of this study are openly available at the following URL/DOI: https://doi.org/10.5281/zenodo.16151579.

Author contributions

Mikita Maslouski 0009-0003-2089-4996
Conceptualization (lead), Data curation (lead), Formal analysis (lead), Investigation (lead), Methodology (lead), Project administration (lead), Resources (lead), Software (lead), Validation (lead), Visualization (lead), Writing – original draft (lead), Writing – review & editing (lead)

Maria Ansari 0009-0007-6785-9417
Data curation (supporting), Investigation (lead), Resources (lead), Validation (equal), Writing – review & editing (equal)

Susanne E Hamburger 0009-0006-0425-8334
Data curation (supporting), Investigation (lead), Resources (lead), Validation (equal), Writing – review & editing (equal)

Johannes Meyer zu Drewer 0000-0003-2619-8417
Data curation (supporting), Investigation (lead), Resources (lead), Validation (equal), Writing – review & editing (equal)

Nikolas Hagemann 0000-0001-8005-9392
Data curation (supporting), Investigation (equal), Resources (equal), Supervision (equal), Validation (equal), Writing – review & editing (lead)

Annette Eschenbach 0000-0002-8778-1342
Investigation (equal), Resources (equal), Supervision (equal), Writing – review & editing (equal)

Christian Beer 0000-0002-5377-3344
Conceptualization (supporting), Supervision (equal), Validation (equal), Writing – review & editing (equal)

Joscha N Becker 0000-0002-3210-3632
Investigation (equal), Resources (equal), Supervision (equal), Validation (equal), Writing – review & editing (equal)

Claudia I Kammann 0000-0001-7477-1279
Investigation (equal), Resources (equal), Supervision (equal), Validation (equal), Writing – review & editing (equal)

Maria-Elena Vorrath 0000-0001-7208-1186
Validation (equal), Writing – review & editing (equal)

Philipp Porada 0000-0002-5072-0220
Conceptualization (lead), Methodology (supporting), Software (supporting), Supervision (lead), Validation (equal), Writing – review & editing (equal)

Appendix A. Model calibration

For all calibration runs, we use meteorological input from local weather station (Hamburger *et al* n.d.). The calibration data are provided with the LiDELSv2 model source in Maslouski and Porada (2025).

A.1. Soil organic carbon (SOC) estimations

In the LiDELSv2 model, the SOC pool increases through the degradation of labile biochar and vegetation inputs simulated by the litter function. This carbon is subsequently processed by soil microbes, which decompose the litter and release carbon as soil CO_2, eventually emitted through soil respiration.

In the Geisenheim experiment (see section 2.1), no litter input occurred, as the entire plant biomass, including roots, was removed after the experiment. However, microbial activity continued, fueled by available SOC and the degradation of the labile biochar fraction.

Biochar was assumed to be applied to a depth of 25 cm, corresponding to the top two modeled soil layers. This depth aligns with the agricultural definition of topsoil (Poeplau *et al* 2020) and matches the pot depth used in the Geisenheim experiment. Carbon release from labile biochar was simulated using a degradation function specific to oak wood biochar produced at 650 °C (Zimmerman 2010):

$$C(t) = C_{\text{in}} \times \left(1 - \frac{\exp(-5.513)}{-0.679 + 1} \cdot t^{-0.679+1} \right)$$

where C_{in} is the initial amount of biochar. This function provided a good fit ($R = 0.97$ pearson correlation coefficient) to the measured SOC values (table A1) and was applied in the LiDELSv2 simulations. In our research, we selected the oak wood biochar decay function because it best matched the data obtained from the Geisenheim experiment, when compared with decay functions for other 650 °C biochars in Zimmerman (2010) and with the function proposed in the Global Biochar C-Sink Standard 3.1 (Schmidt *et al* 2024).

The above function predicts that about 88% of the initially applied oak biochar would remain after 1000 years. To ensure consistency with the assumed PAC fraction of the (RE-)biochar, we constrained the decay curve such that degradation ceases once the PAC limit is reached, which occurs after approximately 500 years in our simulations.

Table A1. Comparison of measured and modeled soil organic carbon (SOC).

Treatment	Measured SOC (%)	Modeled SOC (%)
Control initial	1.24	—
Control final	1.17	1.17
Rock powder (RP)	1.13	1.21
Wood biochar (WB)	1.98	1.89
Co-application RP + WB	1.84	1.84
Co-pyrolysis (RE-biochar)	1.96	1.78

A.2. Soil MB as a function of SOC

An empirical power-law relationship was derived from the data fit, using the functional form and coefficient proposed by Liddle *et al* (2020):

$$\text{MB} \left(\text{mg kg}^{-1} \right) = 432 \times 10^{0.00815 \times \text{SOC} \left(\text{g kg}^{-1} \right)}.$$

This function was then used to predict MB for the measurement samples based on measured SOC values (table A2). A regression fitted to the measured MB values yielded the following relationship:

$$\text{Measured MB} = 1.5 \times \text{Modeled MB} - 190.05$$

with a Pearson correlation coefficient of $R = 0.93$. Based on this calibration, the final equation used in the model was:

$$\text{MB} \left(\text{mg kg}^{-1} \right) = 648 \times 10^{0.00815 \times \text{SOC} \left(\text{g kg}^{-1} \right)} - 190.05$$

Table A2. Measured soil organic carbon (SOC) and microbial biomass (MB) from Ansari *et al* (n.d.), compared to modeled MB based on the relationship proposed by Liddle *et al* (2020).

Parameter treatment	Measured SOC (g kg^{-1})	Measured MB (mg kg^{-1})	Modeled MB (mg kg^{-1})
Control	12	622	539
Rock powder (RP)	11	589	534
Wood biochar (WB)	20	754	627
Co-application RP + WB	18	730	611
Co-pyrolysis (RE-biochar)	20	712	624

A.3. Net primary production (NPP)

NPP in LiDELS is represented as a CO_2 assimilation process, limited by light availability and atmospheric CO_2 concentration. Vegetation growth is also influenced by soil water availability.

In the Geisenheim experiment (see section 2.1), plant yields as well as leaf and root dry biomass were measured (table A3). Modeled NPP accounts for approximately 25% of the measured dry biomass, which is lower than expected based on literature values of 38%–46% (Pate and Layzell 1981). Despite a good fit between modeled NPP and measured dry yields ($R = 0.79$, Pearson correlation coefficient), this discrepancy may be explained by the LiDELS model not accounting for the nutrient-enhancing effects of biochar–rock applications, which can significantly promote plant growth. In the Geisenheim experiment, plants were additionally fertilized with both mineral (Ferty 2 Mega) and organic (Vinasse CARBUNA AND) fertilizers—an effect not represented in the model. Furthermore, the vegetation parameters in the model may not be optimized for the specific crop used in the experiment; instead, LiDELS simulates a generic C3 plant rather than the cabbage turnip cultivated in the study.

To assess model dynamics, we calculated the correlation between measured dry yields and the mean soil water content simulated by the model (table A3), which showed a strong relationship ($R = 0.82$, Pearson correlation coefficient). The correlation between modeled NPP and mean soil water content was even higher, with $R = 0.97$.

Table A3. Measured dry biomass from Hamburger *et al* (n.d.), compared to modeled net primary production (NPP) and modeled mean soil water content in the 25 cm soil column, representing the pot depth used in the lysimeter experiment by Hamburger *et al* (n.d.).

Parameter Treatment	Mean soil water content (—)	NPP (g C m^{-2})	Dry biomass (g m^{-2})
Control	0.186	313	1170
Rock powder (RP)	0.190	314	1167
Wood biochar (WB)	0.205	319	1351
Co-application RP + WB	0.209	321	1301
Co-pyrolysis (RE-biochar)	0.197	316	1203

Appendix B.

Figure B1. Simplified representation of the updated LiDELSv2 model structure. New processes and connections introduced compared to the previous release in Maslouski *et al* (2025) are highlighted in blue. Angle brackets $\langle\rangle$ denote vector-valued variables defined for each soil layer. R_{net} represents net radiation at the soil surface. T indicates temperature at the surface ($_{surf}$) or within soil layers. ET refers to evapotranspiration, either potential ($_{pot}$) or actual, while E refers to evaporation. R denotes CO_2 respiration from the entire plant ($_d$) or from the soil. CO_2 indicates gas concentration in the air or within soil layers. Q_b refers to seepage. θ is the soil water content, and I is the soil ice content. d specifies soil layer thickness. The parameter c describes the vertical distribution of soil organic matter ($_o$), MB ($_m$), or root biomass ($_r$). $[Ca^{2+}]$ referes to the leaching rate of calcium ions. Reproduced from Maslouski *et al* (2025). © The Author(s). Published by IOP Publishing Ltd. CC BY 4.0.

References

Acharya B S, Dodla S, Wang J J, Pavuluri K, Darapuneni M, Dattamudi S, Maharjan B and Kharel G 2024 Biochar impacts on soil water dynamics: knowns, unknowns and research directions *Biochar* **6** 34

Al-Ghussain L 2019 Global warming: review on driving forces and mitigation *Environ. Prog. Sustain. Energy* **38** 13–21

Altdorff D, Galagedara L, Abedin J and Unc A 2019 Effect of biochar application rates on the hydraulic properties of an agricultural-use boreal podzol *Soil Syst.* **3** 53

Amann T and Hartmann J 2019 Ideas and perspectives: synergies from co-deployment of negative emission technologies *Biogeosciences* **16** 2949–60

Ansari M, Stock S, Dippold M, Hamburger S E, Kammann C, Meyer zu Drewer J, Hagemann N, Eschenbach A and Becker J N n.d. Biochar dominated the combined effect of silicate rock powder and biochar application on extracellular enzyme kinetics and nutrient dynamics in a sandy soil *Soil Till. Res.* submitted

Antonangelo J A, Culman S and Zhang H 2024 Comparative analysis and prediction of cation exchange capacity via summation: influence of biochar type and nutrient ratios *Front. Soil Sci.* **4** 1371777

Archontoulis S V, Huber I, Miguez F E, Thorburn P J, Rogovska N and Laird D A 2016 A model for mechanistic and system

assessments of biochar effects on soils and crops and trade-offs *Glob. Change Biol. Bioenergy* **8** 1028–45

Arens S 2013 Global limits on silicate weathering and implications for the silicate weathering feedback *PhD Thesis* Friedrich-Schiller-Universität Jena (available at: www.db-thueringen.de/receive/dbt_mods_00023499)

Arens S and Kleidon A 2008 Global sensitivity of weathering rates to atmospheric CO_2 under the assumption of saturated river discharge *Mineral. Mag.* **72** 301–4

Arens S and Kleidon A 2011 Eco-hydrological versus supply-limited weathering regimes and the potential for biotic enhancement of weathering at the global scale *Appl. Geochem.* **26** S274–8

Beerling D J *et al* 2020 Potential for large-scale CO_2 removal via enhanced rock weathering with croplands *Nature* **583** 242–8

Bekchanova M, Kuppens T, Cuypers A, Jozefczak M and Malina R 2024 Biochar's effect on the soil carbon cycle: a rapid review and meta-analysis *Biochar* **6** 88

Blanco-Canqui H 2017 Biochar and soil physical properties *Soil Sci. Soc. Am. J.* **81** 687–711

Blanco-Canqui H, Laird D A, Heaton E A, Rathke S and Acharya B S 2020 Soil carbon increased by twice the amount of biochar carbon applied after 6 years: field evidence of negative priming *Glob. Change Biol. Bioenergy* **12** 240–51

Bonan G 2019 *Climate Change and Terrestrial Ecosystem Modeling* (Cambridge University Press) (https://doi.org/10.1017/9781107339217)

Buss W, Wurzer C, Manning D A C, Rohling E J, Borevitz J and Mašek O 2022 Mineral-enriched biochar delivers enhanced nutrient recovery and carbon dioxide removal *Commun. Earth Environ.* **3** 67

Calvin K *et al* 2023 IPCC, 2023: climate change 2023: synthesis report, summary for policymakers *Contribution of Working Groups I, II and III to the Sixth Assessment Report of the Intergovernmental Panel on Climate Change* (IPCC) pp 1–34

Chiaravalloti I, Theunissen N, Zhang S, Wang J, Sun F, Ahmed A A, Pihlap E, Reinhard C T and Planavsky N J 2023 Mitigation of soil nitrous oxide emissions during maize production with basalt amendments *Front. Clim.* **5** 1203043

Ciais P *et al* (Carboeurope Synthesis Team) 2010 The European carbon balance. Part 2: croplands *Glob. Chang. Biol.* **16** 1409–28

Dietzen C, Harrison R and Michelsen-Correa S 2018 Effectiveness of enhanced mineral weathering as a carbon sequestration tool and alternative to agricultural lime: an incubation experiment *Int. J. Greenhouse Gas Control* **74** 251–8

Meyer zu Drewer J *et al* 2025 Pyrogenic carbon and carbonating minerals for carbon capture and storage (PyMiCCS) part I: production, physico-chemical characterization and C-sink potential *Front. Clim.* **7** 1631368

Dupla X, Claustre R, Bonvin E, Graf I, Le Bayon R C and Grand S 2024 Let the dust settle: impact of enhanced rock weathering on soil biological, physical and geochemical fertility *Sci. Total Environ.* **954** 176297

Dupla X, Möller B, Baveye P C and Grand S 2023 Potential accumulation of toxic trace elements in soils during enhanced rock weathering *Eur. J. Soil Sci.* **74** e13343

Farquhar G D, von Caemmerer S and Berry J A 1980 A biochemical model of photosynthetic CO_2 assimilation in leaves of C3 species *Planta* **149** 78–90

Grafmüller J, Möllmer J, Muehe E M, Kammann C I, Kray D, Schmidt H P and Hagemann N 2024 Granulation compared to co-application of biochar plus mineral fertilizer and its impacts on crop growth and nutrient leaching *Sci. Rep.* **14** 16555

Gross A, Bromm T and Glaser B 2021 Soil organic carbon sequestration after biochar application: a global meta-analysis *Agronomy* **11** 2474

Gross A, Bromm T, Polifka S, Fischer D and Glaser B 2024 Long-term biochar and soil organic carbon stability—evidence from field experiments in germany *Sci. Total Environ.* **954** 176340

Guo F, Wang C, Wang S, Zhao X, Li G and Sun Z 2024 The native SOC increase in woodland and lawn soil amended with biochar surpassed greenhouse—a seven-year field trial *Sci. Total Environ.* **907** 167924

Hagemann N, Schmidt H P, Bucheli T D, Grafmüller J, Vosswinkel S, Herdegen V, Meredith W, Uguna C N and Snape C E 2025 Proxies for use in biochar decay models: hydropyrolysis, electric conductivity and H/Corg molar ratio *PLoS One* **20** e0330206

Hamburger S E, Görres C M, Hagemann N, Meyer zu Drewer J, Ansari M, Geilfus C M and Kammann C n.d. The effects of biochar in combined application with rock powder on agricultural parameters and on soil greenhouse gas emission (in preparation)

Han M *et al* 2024 Modeling biochar effects on soil organic carbon on croplands in a microbial decomposition model (MIMICS-BC_v1.0) *Geosci. Model Dev.* **17** 4871–90

Hartmann J, West A J, Renforth P, Köhler P, De La Rocha C L, Wolf-Gladrow D A, Dürr H H and Scheffran J 2013 Enhanced chemical weathering as a geoengineering strategy to reduce atmospheric carbon dioxide, supply nutrients and mitigate ocean acidification *Rev. Geophys.* **51** 113–49

Hersbach H *et al* 2020 The ERA5 global reanalysis *Q. J. R. Meteorol. Soc.* **146** 1999–2049

Honvault N, Tiouchichine M L, Sauze J, Piel C, Landais D, Devidal S, Gritti E, Bosch D and Milcu A 2024 Additive effects of basalt enhanced weathering and biochar co-application on carbon sequestration, soil nutrient status

and plant performance in a mesocosm experiment *Appl. Geochem.* **169** 106054

Howell A, Helmkamp S and Belmont E 2022 Stable polycyclic aromatic carbon (SPAC) formation in wildfire chars and engineered biochars *Sci. Total Environ.* **849** 157610

Jiang Z, Huang S and Meng Z 2025 Long-term effects of biochar on the hydraulic properties of soil: a meta-analysis based on 1–10 years field experiments *Geoderma* **458** 117318

Joseph S *et al* 2021 How biochar works and when it doesn't: a review of mechanisms controlling soil and plant responses to biochar *Glob. Change Biol. Bioenergy* **13** 1731–64

Keerthi M M 2024 Innovative approaches to carbon sequestration emerging technologies and global impacts on climate change mitigation *Environ. Rep.* **6** 15–18

Kujawska J 2023 Content of heavy metals in various biochar and assessment environmental risk *J. Ecol. Eng.* **24** 287–95

Lawrence D M and Slater A G 2008 Incorporating organic soil into a global climate model *Clim. Dyn.* **30** 145–60

Lee M H, Chang E H, Lee C H, Chen J Y and Jien S H 2021 Effects of biochar on soil aggregation and distribution of organic carbon fractions in aggregates *Processes* **9** 1431

Lehmann J, Cowie A, Masiello C A, Kammann C, Woolf D, Amonette J E, Cayuela M L, Camps-Arbestain M and Whitman T 2021 Biochar in climate change mitigation *Nat. Geosci.* **14** 883–92

Li Z L *et al* 2021 Changes in net ecosystem exchange of CO_2 in Arctic and their relationships with climate change during 2002–2017 *Adv. Clim. Chang. Res.* **12** 475–81

Liddle K, McGonigle T and Koiter A 2020 Microbe biomass in relation to organic carbon and clay in soil *Soil Syst.* **4** 41

Ma L 2020 Effects of spatial-temporal land cover distribution on gross primary production and net primary production in Schleswig-Holstein, northern Germany *Carbon Balance Manage.* **15** 3

Maslouski M, Eschenbach A, Beer C, Thomsen S and Porada P 2025 Soil and vegetation responses to biochar application in terms of its feedback on carbon sequestration under different environmental conditions—LiDELS model overview *Environ. Res. Lett.* **20** 044020

Maslouski M and Porada P 2024 *LiBry-DETECT Layer Scheme Model* (https://doi.org/10.5281/zenodo.14849558)

Maslouski M and Porada P 2025 *LiBry-DETECT Layer Scheme Model v2* (https://doi.org/10.5281/zenodo.16151579)

Meyer zu Drewer J and Hagemann N 2025 *Industrial Production and Characterization of Biochar and Rock-Enhanced Biochar [Data set]* (https://doi.org/10.5281/zenodo.15840176)

Mia S, Dijkstra F A and Singh B 2017 Long-term aging of biochar *Adv. Agron.* **141** 1–51

Miralles D G *et al* 2025 GLEAM4: global land evaporation and soil moisture dataset at 0.1 resolution from 1980 to near present *Sci. Data* **12** 416

Nockolds S R 1954 Average chemical compositions of some igneous rocks *Geol. Soc. Am. Bull.* **65** 1007

Obia A, Børresen T, Martinsen V, Cornelissen G and Mulder J 2017 Effect of biochar on crust formation, penetration resistance and hydraulic properties of two coarse-textured tropical soils *Soil Till. Res.* **170** 114–21

Pate J S and Layzell D B 1981 Carbon and nitrogen partitioning in the whole plant—a thesis based on empirical modeling *Nitrogen and Carbon Metabolism* (Springer Netherlands) pp 94–134

Poeplau C, Jacobs A, Don A, Vos C, Schneider F, Wittnebel M, Tiemeyer B, Heidkamp A, Prietz R and Flessa H 2020 Stocks of organic carbon in German agricultural soils—Key results of the first comprehensive inventory *J. Plant Nutr. Soil Sci.* **183** 665–81

Porada P, Weber B, Elbert W, Pöschl U and Kleidon A 2013 Estimating global carbon uptake by lichens and bryophytes with a process-based model *Biogeosciences* **10** 6989–7033

Renforth P and Henderson G 2017 Assessing ocean alkalinity for carbon sequestration *Rev. Geophys.* **55** 636–74

Ryan E M, Ogle K, Kropp H, Samuels-Crow K E, Carrillo Y and Pendall E 2018 Modeling soil CO_2 production and transport

with dynamic source and diffusion terms: testing the steady-state assumption using DETECT v1.0 *Geosci. Model Dev.* **11** 1909–28

Schmidt H P, Anca-Couce A, Hagemann N, Werner C, Gerten D, Lucht W and Kammann C 2019 Pyrogenic carbon capture and storage *Glob. Change Biol. Bioenergy* **11** 573–91

Schmidt H P, Kammann C and Hagemann N 2024 *Global Biochar C-Sink Standard* (available at: www.carbon-standards.com/docs/transfer/4000039EN.pdf) (Accessed 1 April 2025)

Schmidt H P, Kammann C, Hagemann N, Leifeld J, Bucheli T D, Sánchez Monedero M A and Cayuela M L 2021 Biochar in agriculture—a systematic review of 26 global meta-analyses *Glob. Change Biol. Bioenergy* **13** 1708–30

Smith S M *et al* 2024 *The State of Carbon Dioxide Removal* 2nd edn (OSF) (https://doi.org/10.17605/OSF.IO/F85QJ)

Swoboda P, Döring T F and Hamer M 2022 Remineralizing soils? The agricultural usage of silicate rock powders: a review *Sci. Total Environ.* **807** 150976

Tomczyk A, Sokołowska Z and Boguta P 2020 Biochar physicochemical properties: pyrolysis temperature and feedstock kind effects *Rev. Environ. Sci. Biotechnol.* **19** 191–215

Vienne A, Poblador S, Portillo-Estrada M, Hartmann J, Ijiehon S, Wade P and Vicca S 2022 Enhanced weathering using basalt rock powder: carbon sequestration, co-benefits and risks in a mesocosm study with Solanum tuberosum *Front. Clim.* **4** 869456

Vitková J, Šurda P, Lichner Ĺ and Výleta R 2024 Influence of biochar application rate, particle size and pyrolysis temperature on hydrophysical parameters of sandy soil *Appl. Sci.* **14** 3472

Vorrath M E *et al* 2025 Pyrogenic carbon and carbonating minerals for carbon capture and storage (PyMiCCS) part II: organic and inorganic carbon dioxide removal in an oxisol *Front. Clim.* **7** 1592454

Wang J, Xiong Z and Kuzyakov Y 2016 Biochar stability in soil: meta-analysis of decomposition and priming effects *Glob. Change Biol. Bioenergy* **8** 512–23

Weng Z H *et al* 2022 Microspectroscopic visualization of how biochar lifts the soil organic carbon ceiling *Nat. Commun.* **13** 5177

Zimmerman A R 2010 Abiotic and microbial oxidation of laboratory-produced black carbon (biochar) *Environ. Sci. Technol.* **44** 1295–301